Engineering Research Journal

journal homepage: https://erj.journals.ekb.eg/

Study of the failure mechanism for footings subjected to tension and lateral loads using digital photogrammetry program (Laboratory Study)

Nourhan Mahmoud[1,*], Amr Radwan[2], Dalia Bahaa[3], Heba Elsaid[4]

[1] Assistant lecturer, Faculty of Engineering at Egyptian Russian University, Cairo, Egypt
[2] Professor of Geotechnical Engineering, Faculty of Engineering at Mataria branch, Helwan University, Cairo, Egypt
[3] Professor of Geotechnical Engineering, Faculty of Engineering at Badr University, Cairo, Egypt
[4]lecturer, Faculty of Engineering at Egyptian Russian University University, Cairo, Egypt

[*]Corresponding author E-mail: norhanmahmoud350@gmail.com

Abstract. This research examines the behavior of shallow footings subjected to vertical load and lateral forces, with a specific focus on the construction of high voltage electrical networks in Egypt. These projects necessitate the installation of thousands of lattice towers of varying shapes and sizes. Given the significant cost associated with foundation works in transmission projects, understanding the pullout resistance of footings is crucial for achieving cost-effective and rational designs. The study investigates the impact of various parameters, including soil type and the ratio of foundation depth to footing width, on the uplift capacity and failure mechanisms of shallow footings under vertical and horizontal forces. A comprehensive a number of laboratory examinations were conducted using footing dimensions of 3.5×7 cm, 5×10 cm, and 7.5×15 cm. Tests were performed at relative densities of 95% and 85%, with foundation depth to footing width ratios of 1, 1.5, and 2.5. Experimental work was carried out in a steel tank with internal dimensions of 0.60×0.40 m in plan and 0.40 m in depth. A digital photogrammetry program was employed to measure the complete displacement field within the soil mass. These techniques provide valuable insights into the behavior of shallow footings under the specified loading conditions, contributing to the optimization of foundation design for transmission projects. By focusing on the parameters that influence the pullout resistance and failure mechanisms of shallow footings, this study aims to improve the understanding and design of foundations for high voltage electrical networks, ensuring both economic efficiency and structural integrity.

Keywords: Lateral force – Uplift resistance– Failure rupture – The angle of inclination.

• Introduction

This paper presents the results and analysis of experimental work conducted on model footings subjected to tension forces and horizontal loads. The primary aim of this study is to understand how footings and the surrounding soil respond in the context of electrical towers. Key design factors for

DOI: 10.21608/erj.2025.343112.1159
Received 09 December 2024; Received in revised form 15 January 2025; Accepted 25 January 2025
Available online 01 March 2025

these types of foundations include the expected uplift capacity and the soil failure mechanism. To achieve these objectives, the study employs photogrammetry techniques to investigate the failure process of footings in various types of sand. The outcomes of the various tests are presented and explained in detail, offering valuable insights into the behavior of footings under the specified loading conditions. By focusing on these aspects, this research contributes to the optimization of foundation designs, ensuring both structural integrity and economic efficiency for projects involving high voltage electrical networks in Egypt.

To address the increasing number of anchorage issues, a variety of anchors have been developed in the field. Among these, plate anchors are considered one of the most widely used types due to their application in numerous onshore and offshore construction and maintenance projects. Plate anchors offer a cost-effective solution for resisting uplift stresses, outperforming gravity-based and other embedded anchors (Bouazza and Finlay, 1990). Numerous studies have focused on the uplift behavior of plate anchors buried in both cohesive and cohesionless soils. This review examines the existing research aimed at predicting the uplift behavior of plate anchors in cohesionless soils under both cyclic and monotonic loading conditions. Through a detailed analysis of the literature, this review provides insights into the factors influencing anchor performance, such as soil type, loading conditions, and anchor design. The findings highlight the importance of understanding these parameters to enhance the design and implementation of plate anchors in various geotechnical applications.

Uplift theories in geotechnical engineering typically rely on the assumption of specific failure surfaces. One of the earliest methodologies was proposed by Marston (1930), who assumed a vertical slip surface with a width equal to the diameter of the submerged pipe. This method provided the first logical approach for calculating loads on buried conduits, taking into account the weight of the soil enclosed by the failure surfaces and the frictional resistance along these surfaces. Despite the theoretical foundation, Marston's assumptions led to behavior that significantly diverged from experimental results and the findings of other researchers. For instance, Trautmann et al. (1985) observed different soil-structure interaction mechanisms under uplift forces, highlighting the limitations and discrepancies in Marston's model. This review emphasizes the need for continued refinement in uplift theories, incorporating experimental data and advanced modeling techniques to better predict soil behavior and uplift resistance in practical applications. The evolution of these theories remains crucial for improving the design and stability of geotechnical structures exposed to uplift forces.

Shichiri et al. (1943) used theoretical and experimental data to establish a method for estimating the uplift capacity of a foundation. He proposed a shearing force along a rupture surface that is vertical. This force is represented by the coefficient of earth pressure at rest, the angle of internal friction, and the cohesiveness of the soil. Majer (1955) estimated the footing's uplift capacity using a straightforward failure mechanism. The pullout capacity was calculated using this method by taking into account the weight of soil within the failure zone and the friction created along the failure surface. The method assumed a cylindrical failure surface with a diameter equal to the anchor width. Mors (1959) made the assumption that a truncated cone extended from the anchor's base to the ground. The weight of the soil mass inside the truncated cone was thought to be equivalent to the anchor's pullout capability. The distinction between shallow and deep anchor failures was not made by either of the previous techniques. For shallow anchors, Mors' cone approach was proven to be conservative; nevertheless, at deeper depths, the opposite was true (Turner 1962). Vesic (1971) used the expansion of cavities in a semi-infinite stiff plastic body to calculate the uplift capacity of embedded objects. The maximum radial pressure required to rupture a spherical or cylindrical hollow was equal to the uplift capacity of the embedded objects.

Numerous studies (Selvadurai 1993; Krishnaswamy and Parashar 1994; Subbarao and Jyanth

Kumar 1994; Swami Saran and Rao 2002; Jyanth Kumar 2004; Subbarao and Manjunatha 2004; Dickin and Laman 2007; Ilamparuthi et al 2002; Kortam 2008; Kumar 2009; Bildik and Laman 2011; Niroumand and Kassim 2013; Emirler et al. 2015; Korkmaz and Keskin 2017; Banerjee S. and Mahadevuni N. 2017 and Heba 2018) have produced a general solution for an anchor plates subjected to uplift force. As a result, this study offers all of the findings and an analysis of the experimental work done on the footing under shear and uplift forces. As previously stated, the goal of this study is to examine how footings and surrounding soil behave in electrical towers, which are frequently subjected to lateral and vertical loads. As a result, the expected uplift capacity and the soil failure mechanism are important design factors for these kinds of foundations. This study uses photogrammetry techniques to investigate the failure process of footings in various types of sand. The results of the various experiments are shown and discussed in this publication. Finally, a summary of the important findings obtained from the experiment is provided.

a) Experimental program

- **Model description**

A sturdy testing tank measuring 60 cm in length, 40 cm in width, and 40 cm in height involves the up the model. **Fig. 1** illustrates the model's components.

A- Perspex plate	B- Steel beam
C- Small wheel	D- wire
E- Weights	F- Footing
G- Vertical angle	H- Horizontal angle

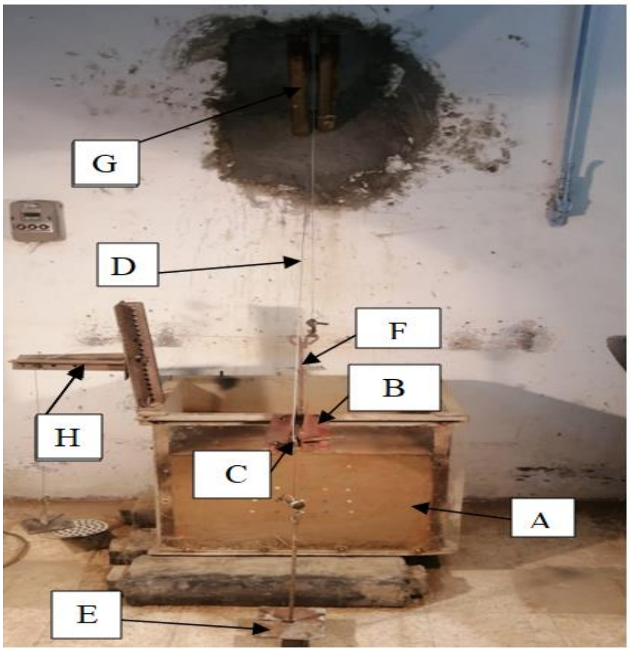

Fig . 1. Photo showing model configuration

1.1 Measurements and measuring system

For this study, a premium digital camera was utilized. The tank's face was 1.2 meters away from where the photos were taken. The camera was set up such that the tank's face and the lens's photographic plane were parallel. Throughout the whole test, the camera was fastened and maintained in place. A remote control was used to take pictures in order to prevent camera vibration. As seen in **Fig. 2**, two 500 watt Tung strum photographic lamps angled 45 degrees to the tank face provided the required light.

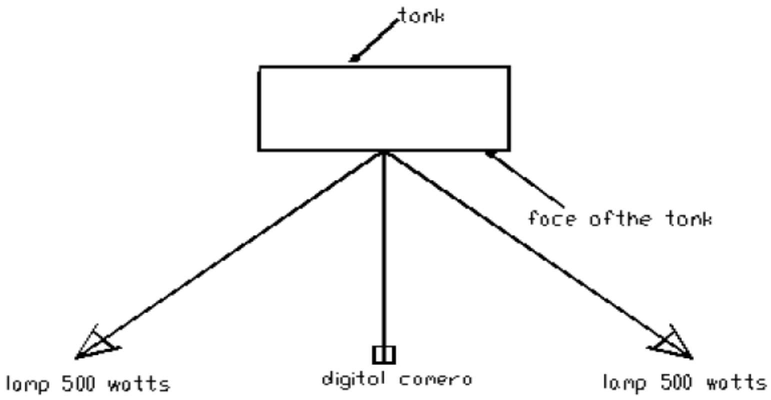

Fig. 2. Set up for photography

Using tracing points in the soil, the test was conducted using the Perspex face to track the gradual growth of soil particle deformation and the failure mechanism of soil and footing based on uplift and lateral force. After the test, the digital photogrammetry technique was utilized to measure the photos that were taken.

b) Test material

Two types of soil are used in the present study. The characteristics of the used soil are given in **Table 1**

Table 1: characteristics of the used soil

Index property	Value
Pure sand	
Specific gravity (Gs)	2.63
D10 (mm)	0.17
Coefficient of uniformity (Cu)	2.61
Coefficient of curvature (Cc)	1.13
Friction angle	36.4º
Maximum dry density	1.802t\m3
Optimum moisture content	6.03%
Sand+8%fines	
Specific gravity (Gs)	2.67
%Coarse	6%
%Silt	23%
%Clay	71%
%Liquid limit	62%-64%

Table 1 cont.: characteristics of the used soil

%Plastic limit	36%-38%
Friction angle	43.1°
Cohesion	0.82t\m2
Soil Classification according to (USCS)	CH

c) Footing plates

- **Considerations:**

The following considerations are taken into account in the choice of the footing plate dimensions :

1. A footing plate with a large size to minimize the effect of the scale errors.
2. The sides of the tank should be sufficiently distant from the footing edges to eliminate their effects on the formation of the failure surface or the truncated mass of soil with the footing.
3. Ayman Lotfy (1992) proved that the maximum dimension for any of the used footing model is chosen not to exceed 100 mm.
4. The ratio between the side length of the container and the maximum dimension of any plate is chosen not to be less than 6.

3.1 Testing procedure

Granular soil compacted to a relative compaction of 95% and 85% was placed in a U-shape at the tank's bottom and lateral sides to create a separate tank sample for each test. Two layers of half of the mixture are added to the tank. A manual rammer is used to compact each layer in order to meet the required unit weight that was established by the compaction tests. A straight wooden rod is used to level the soil's surface.

After excavating the footing location and compacting the soil above it, the footings were placed there and the ground was leveled. Following the completion of the footing preparation, the loading system is fixed; as seen in **Fig.1**, the footing is loaded vertically gradually by placing loads incrementally on the loading system at constant rates that change at different stages. We commit by this loading ratio (6:1) vertical to horizontal, which is the ratio we expected from the proposed tower in Horizon Consulting Engineering, when the footing is subjected to both vertical and horizontal load combined. The final step involved positioning a tripod-mounted digital camera in front of the viewing window and during the testing; photos were taken to enable measurements of footing and foundation soil displacements as shown in **fig.3**.

Fig.3. Final set up test

C) Results and discussion

3.2 Experimental work results for footing under vertical force and lateral force.

3.2.1 The impact of changes of embedment depth of footing -to-footing width (D/B) on the pullout loads for footings subjected to both horizontal and vertical forces.

Where soil type, footing dimension, and relative compaction of soil are constant, the ratio between embedded depth of footing-to-footing width (D\B) (1, 1.5and 2.5) were used.

Tests using different (D/B) were carried out in order to investigate the impact of embedded depth of footing (D) on the ultimate pullout force. There were three different D/B ratios: 1, 1.5, and 2.5.The width of the footing (B) divided by the thickness of the sand layer (D) above the foundation level.

Fig 4 through 6 show how the final pullout force varies with the ratio of embedded depth to footing width. It is apparent after looking at the figures that the ultimate pullout force increases as the footings' embedment depth in the soil increases relative to their width.

The increase in the value of pullout force is for this reason:

- As the depth increases, the quantity of soil involved in resisting the pull increases. In the case of foundations subject to tension, a large part of the resistance is represented due to the weight of soil above the footing. Therefore, as the depth increases, the resistance increases.

- In the case of foundations exposed to both horizontal and vertical forces, the effect of these forces results in its overturning, and thus the foundations begin to resist overturning through friction along the perimeter of the failure plane, which is from the level of the ground's surface up to the level of the foundations. Therefore, the greater in the foundation depth, the greater in the distance of resistance.

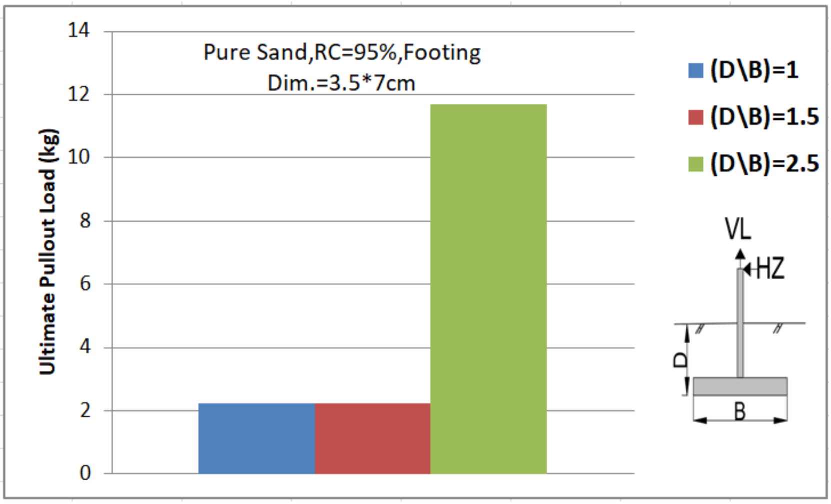

Fig.4. Under tension and lateral forces, the ultimate pullout load varied with (D\B) of footing dimension (3.5*7) cm in pure sand with (RC=95%).

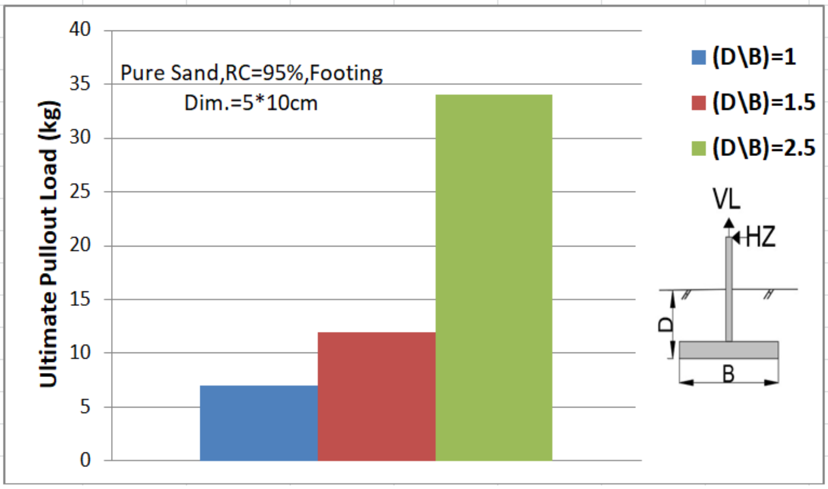

Fig. 5. Under tension and lateral forces, the ultimate pullout load varied with (D\B) of footing dimension (5*10) cm in pure sand with (RC=95%).

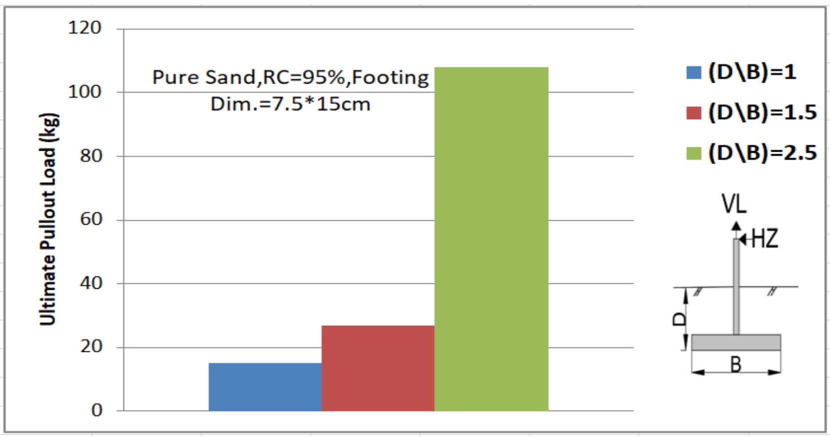

Fig. 6. Under tension and lateral forces, the ultimate pullout load varied with (D\B) of footing dimension (7.5*15) cm in pure sand with (RC=95%).

3.2.2 Impact of changes in the footing's embedment depth to footing width (D\B) on the failure mechanism when subjected to lateral and tensile forces.

By examining **Fig. (7 to24),** the following was concluded:

a. In the case of the embedded depth of footing to footing width (D\B= 1 and 1.5) for all different footing dimensions, the failure shape of soil above footing is the same. It is unsymmetrical inclination, where the angle of inclination (β1) between the vertical line and the failure line in the same direction of the wind, but the angle of inclination (β2) between the vertical line and the failure line in the opposite direction of the wind. In the case of using pure sand, the magnitude of angle (β1) is usually does not depend on angle of internal friction .it is range (30º:45º) in the value. but, the magnitude of angle (β2) is usually given as a function of the angle of internal friction (φ). it often ranges between (0.67: 0.8) from angle of internal friction (φ) as suggested by Fattah and Macky (1992).

b. In the case of the embedded depth of footing to footing width (D\B=2.5) for all different footing dimensions, the rupture surface of soil above footing is the same. It is vertical then unsymmetrical inclination, in the case of using pure sand for all different footing dimensions, the magnitude of angle (β1) is usually ranges between (25º: 40º), the angle (β2) is usually does not depend on angle of internal friction .it is range (15º:30º).

c. In the case of using sand +8% fines with all different embedded depth of footing to footing width (D\B= 1 ,1.5& 2.5) for all different footing dimensions, the failure shape of soil above footing is the same. It is unsymmetrical inclination, the angle (β1) is usually does not depend on angle of internal friction (φ). It often ranges between (45º: 65º), but the angle (β2) is usually does not depend on angle of internal friction .it is range (35º:50º).

In the finally, we can conclude the following that the change in the embedded depth of footing-to-footing width (D\B) up to a depth of 1.5 in pure sand soil has no effect on the shape of the failure mechanism or on the angle of inclination. When the depth increases beyond 1.5, the shape of the failure mechanism changes, becoming vertical, then an unsymmetrical inclination, and the value of the slope angle decreases. However, in the case of sandy soil with a percentage of fines, there is no effect of changing the embedded depth of footing to footing width on both the shape of the failure mechanism and the angle of inclination.

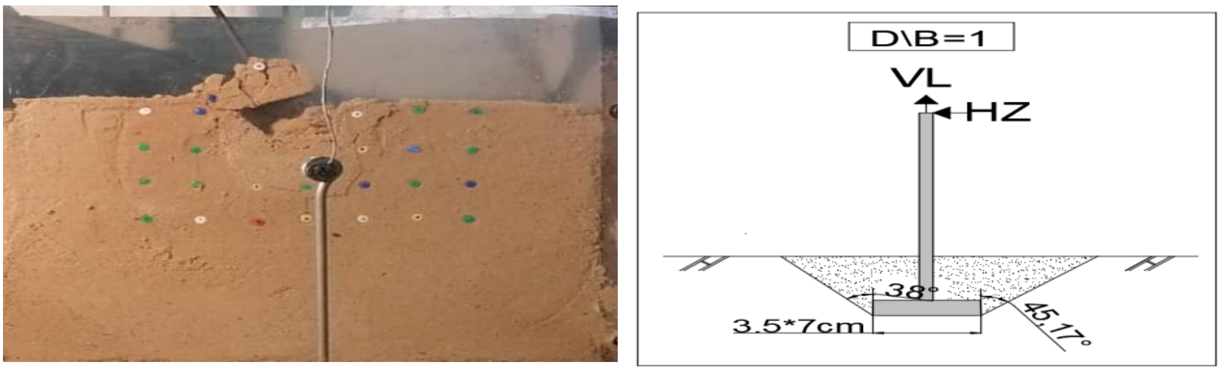

(a) **(b)**

Fig. 7 (a),(b). Failure mechanism for (D\B)=1 of footing dim.(3.5*7)cm in pure sand with (RC=95%) under vertical force and horizontal force.

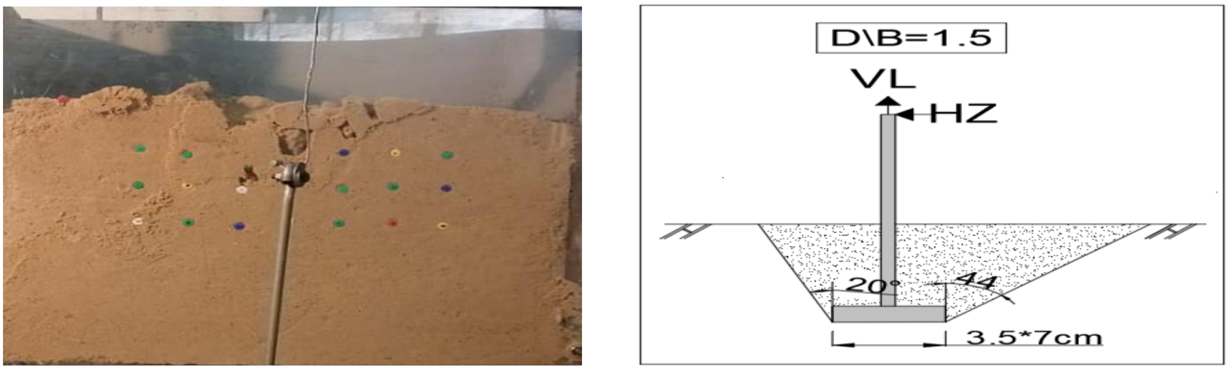

(a)

Fig. 8 (a),(b). Failure mechanism for (D\B)=1.5 of footing dim.(3.5*7)cm in pure sand with (RC=95%) under vertical force and horizontal force.

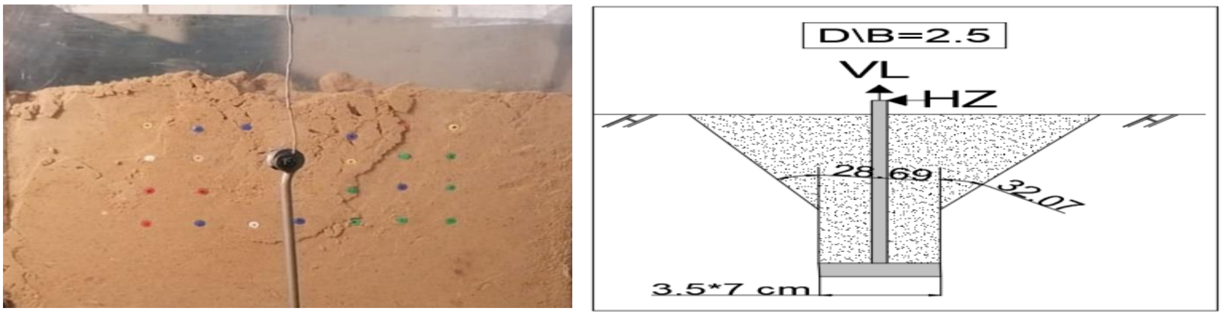

(a) **(b)**

Fig. 9 (a),(b). Failure mechanism for (D\B)=2.5 of footing dim.(3.5*7)cm in pure sand with (RC=95%) under vertical force and horizontal force.

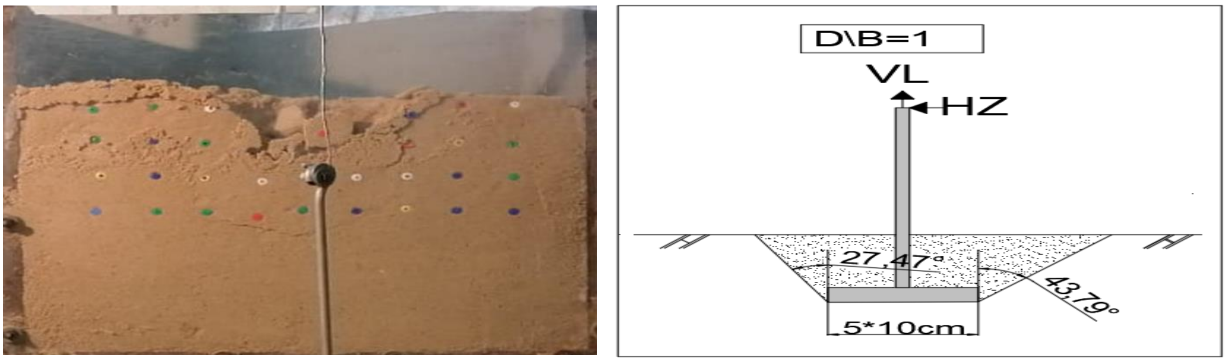

(a) **(b)**

Fig. 10 (a),(b). Failure mechanism for (D\B)=1 of footing dim.(5*10)cm in pure sand with (RC=95%) under vertical force and horizontal force.

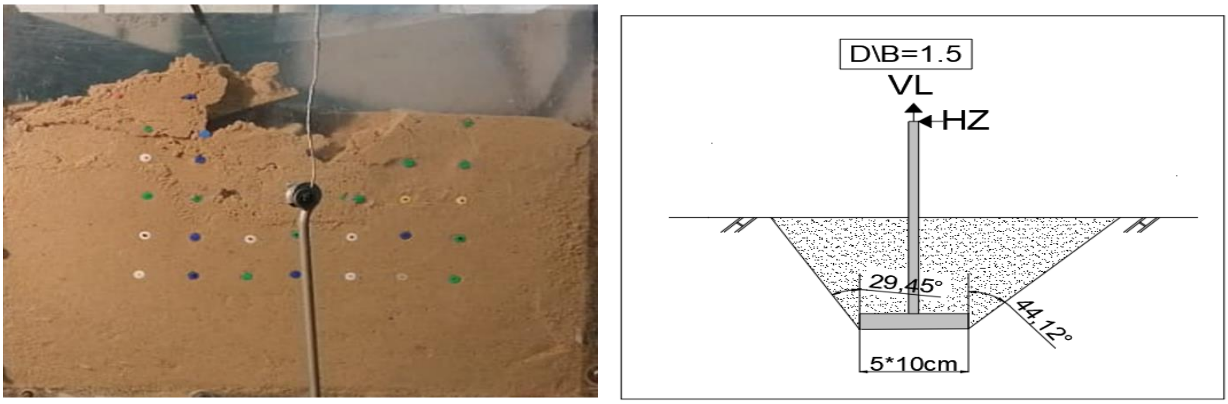

(a)

Fig. 11 (a),(b). Failure mechanism for (D\B)=1.5 of footing dim.(5*10)cm in pure sand with (RC=95%) under vertical force and horizontal force.

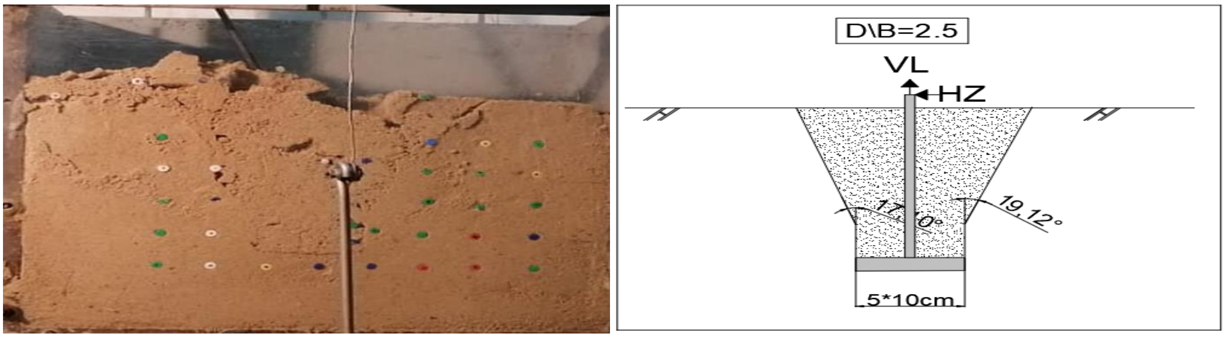

(a)

Fig. 12 (a),(b). Failure mechanism for (D\B)=2.5 of footing dim.(5*10)cm in pure sand with (RC=95%) under vertical force and horizontal force.

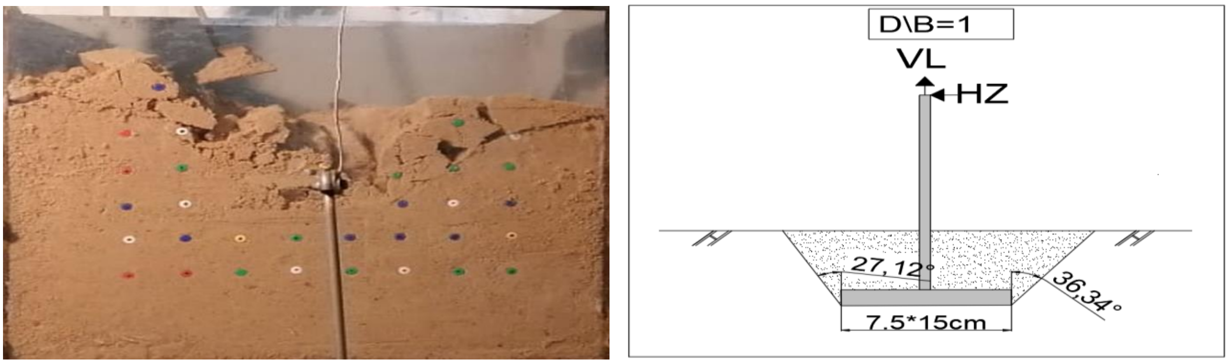

(a)

Fig. 13 (a),(b). Failure mechanism for (D\B)=1 of footing dim.(7.5*15)cm in pure sand with (RC=95%) under vertical force and horizontal force.

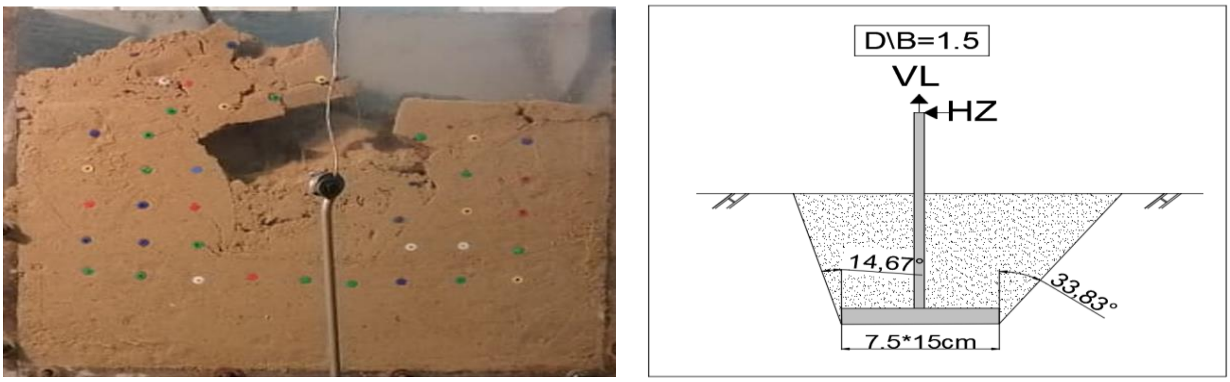

(a)

Fig. 14 (a),(b). Failure mechanism for (D\B)=1.5 of footing dim.(7.5*15)cm in pure sand with (RC=95%) under vertical force and horizontal force.

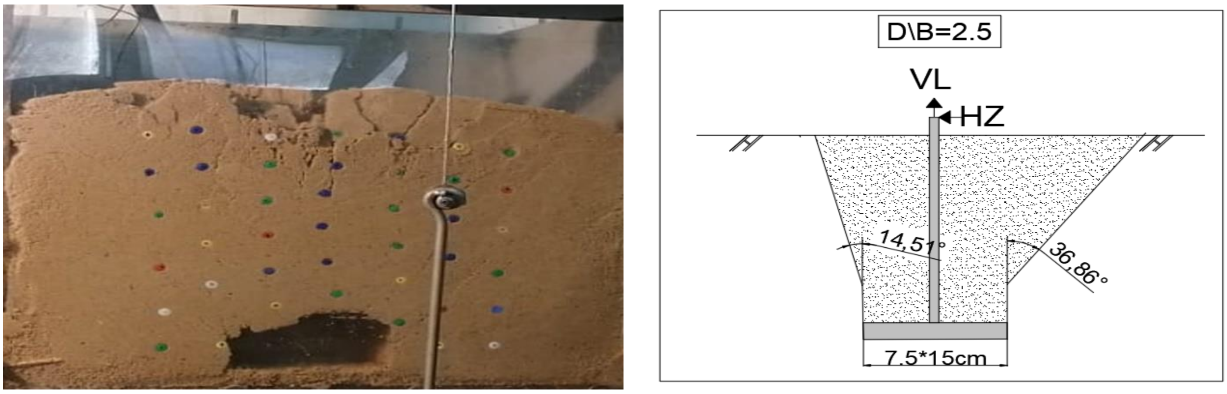

(a)

Fig. 15 (a),(b). Failure mechanism for (D\B)=2.5 of footing dim.(7.5*15)cm in pure sand with (RC=95%) under vertical force and horizontal force.

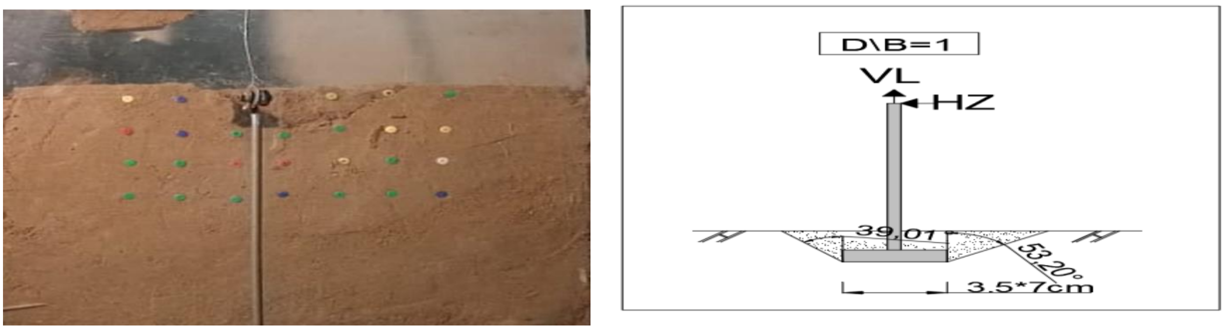

(a)

Fig. 16 (a),(b). Failure mechanism for (D/B)=1 of footing dim.(3.5*7)cm in sand +8%fines with (RC=95%) under vertical force and horizontal force.

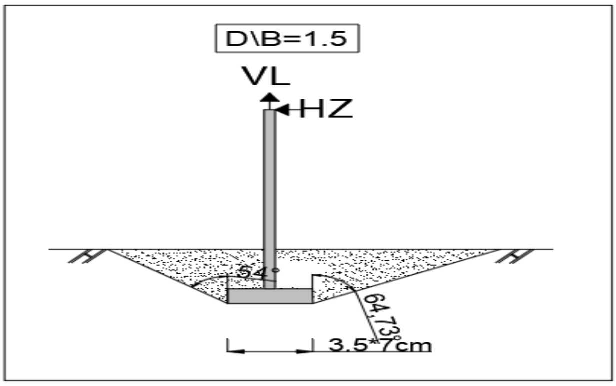

(a)

Fig. 17 (a),(b). Failure mechanism for (D/B)=1.5 of footing dim.(3.5*7)cm in sand +8%fines with (RC=95%) under vertical force and horizontal force.

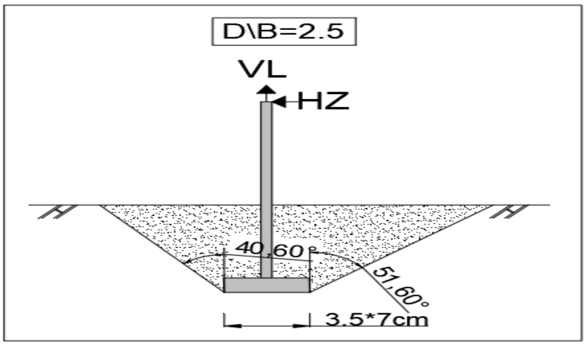

(a) (b)

Fig. 18 (a),(b). Failure mechanism for (D/B)=2.5 of footing dim.(3.5*7)cm in sand +8%fines with (RC=95%) under vertical force and horizontal force.

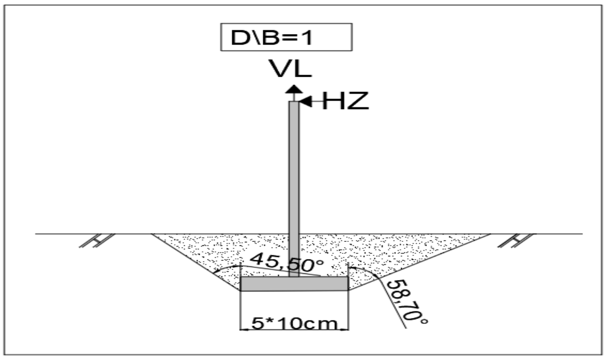

(a) (b)

Fig. 19 (a),(b). Failure mechanism for (D/B)=1 of footing dim.(5*10)cm in sand +8%fines with (RC=95%) under vertical force and horizontal force.

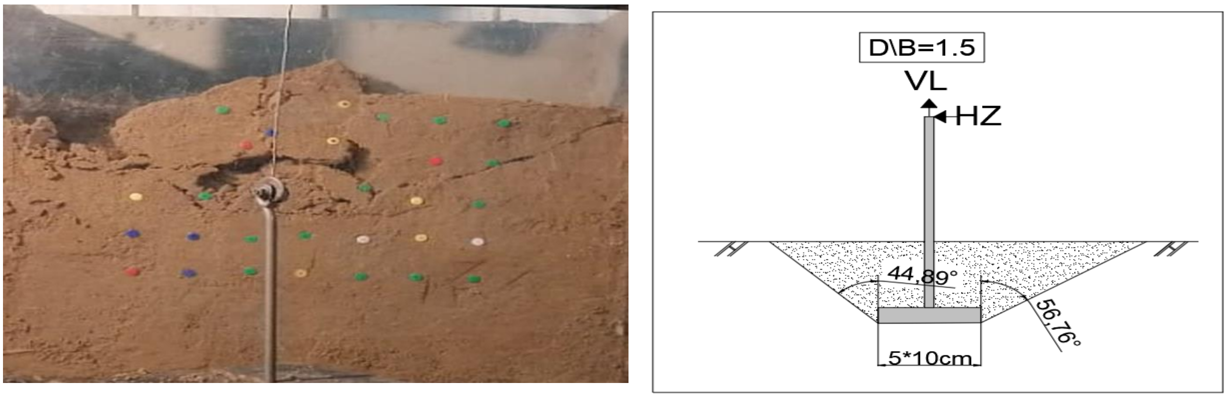

(a) **(b)**

Fig. 20 (a),(b). Failure mechanism for (D/B)=1.5 of footing dim.(5*10)cm in sand +8%fines with (RC=95%) under vertical force and horizontal force.

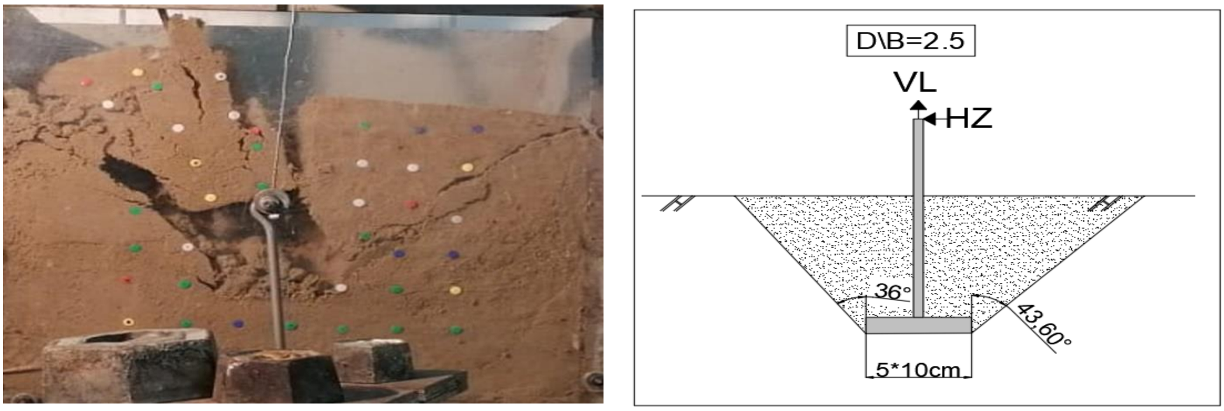

(a) **(b)**

Fig. 21 (a),(b). Failure mechanism for (D/B)=2.5 of footing dim.(5*10)cm in sand +8%fines with (RC=95%) under vertical force and horizontal force.

(a) **(b)**

Fig 22 (a),(b). Failure mechanism for (D/B)=1 of footing dim.(7.5*15)cm in sand +8%fines with (RC=95%) under vertical force and horizontal force.

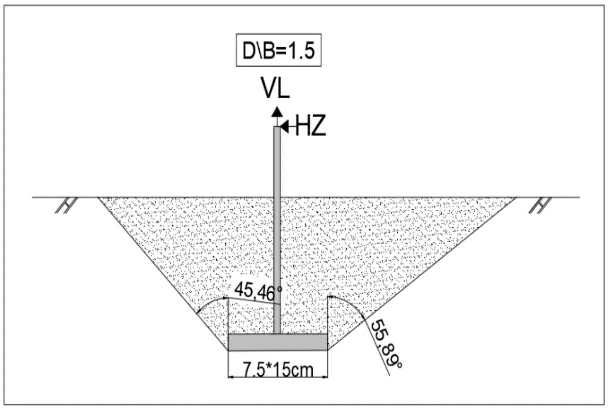

(a) **(b)**

Fig. 23 (a),(b). Failure mechanism for (D/B)=1.5 of footing dim.(7.5*15)cm in sand +8%fines with (RC=95%) under vertical force and horizontal force.

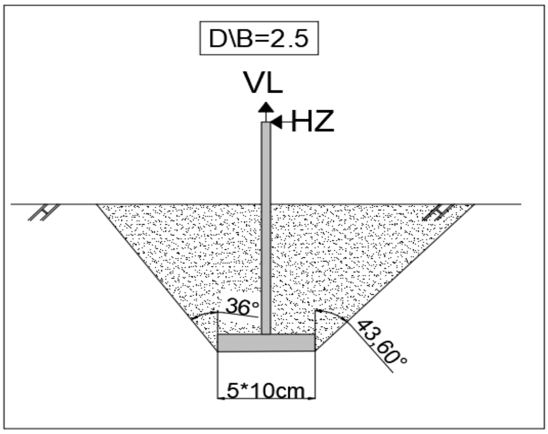

(a) **(b)**

Fig. 24 (a),(b). Failure mechanism for (D/B)=2.5 of footing dim.(7.5*15)cm in sand +8%fines with (RC=95%) under vertical force and horizontal force.

Pure sand and sand + 8% fines are the soil types utilized when the footing dimension, relative compaction, and the ratio of embedded depth of footing to footing width (D\B) are all constant.

The variation of ultimate pullout loads versus soil type is shown in **Fig. 25 through 27.** It is observed that when the soil type is sand + 8% fines, the final pullout force value is greater than when the soil type is pure sand.

The increase in the value of pullout force is because the presence of a percentage of fines in the soil improves the properties of the soil (shear strength parameters) which leads to friction developed along the failure surface, and also improvement in the cohesion forces between the particles and the footing.

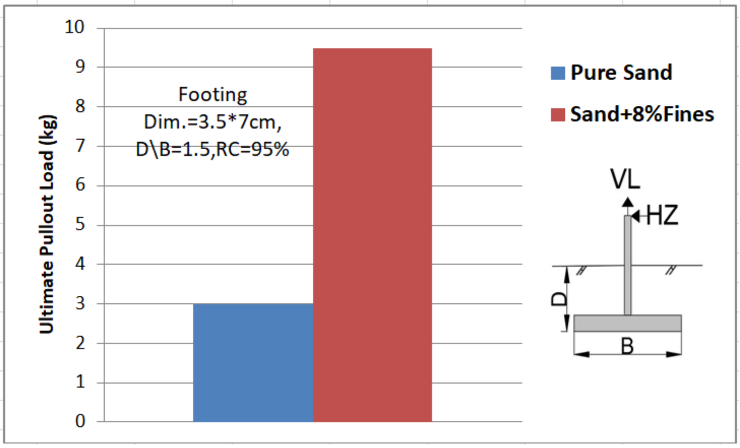

Fig. 25. With varying soil types (pure sand and sand plus 8% fines), the ultimate pullout load varies with footing dimensions (3.5*7) cm, (D/B)=1.5, and (RC=95%) under both vertical and horizontal forces.

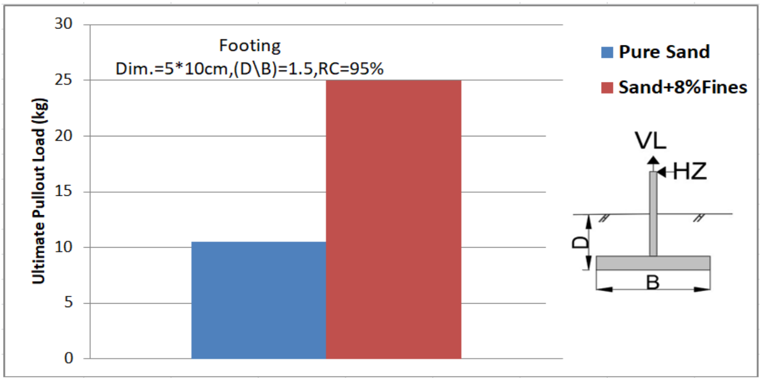

Fig. 26. With varying soil types (pure sand and sand plus 8% fines), the ultimate pullout load varies with footing dimensions (5*10) cm, (D/B)=1.5, and (RC=95%) under both vertical and horizontal forces.

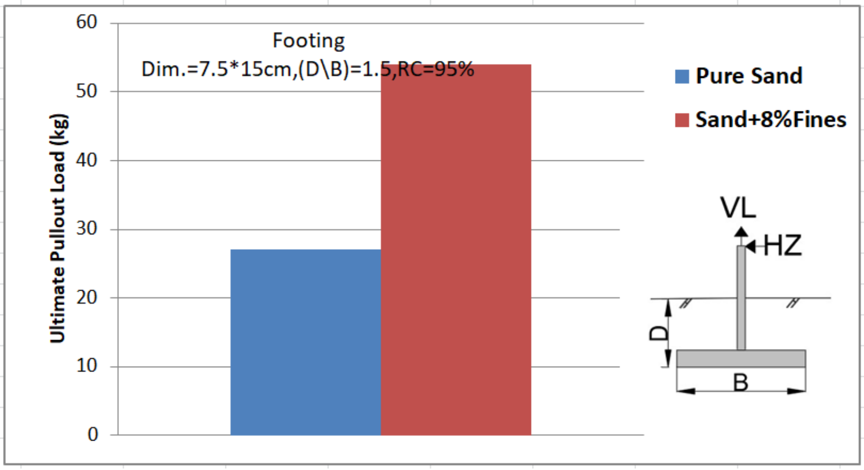

Fig. 27. With varying soil types (pure sand and sand plus 8% fines), the ultimate pullout load varies with footing dimensions (7.5*15) cm, (D/B)=1.5, and (RC=95%) under both vertical and horizontal forces.

3.2.3 The impact of soil type variation on the mechanism of failure under lateral and tension forces.

By examining **Fig. 28 to 32** the following was concluded:

a. In the case of using pure sand, the embedded depth of footing to footing width (D\B= 1 and 1.5) for all different footing dimensions, the failure shape of soil above footing the same. It is unsymmetrical inclination, where the angle of inclination (β1) often ranges between (30º:45º) and the angle (β2) is usually given as a function of the angle of internal friction (φ). It often ranges between (0.67: 0.8) from angle of internal friction (φ) but when the embedded depth of footing to footing width (D\B)=2.5 the failure mechanism is vertical then unsymmetrical inclination. The angle of inclination (β) often ranges between (0.67: 0.8) from angle of internal friction (φ) for footing dimension (3.5*7&5*10) cm but for footing dimension (7.5*15) cm the angle of inclination is usually does not depend on angle of internal friction (φ) it is range (15º:17º).

b. In the case of using sand +8% fines with all different embedded depth of footing to footing width (D\B= 1 ,1.5& 2.5) for all different footing dimensions, the failure shape of soil above footing is the same. It is unsymmetrical inclined, the angle (β1) is usually does not depend on angle of internal friction (φ). It often ranges between (45º: 65º), but the angle (β2) is usually does not depend on angle of internal friction .it is range (35º:50º).

The increase in the value of the angle of inclination (β) in the case using sand+8%fines more than using pure sand is for this reason:

- The strength of the sand+8%fines is more than pure sand, so the soil mass with which it resists increases and thus the angle of inclination (β) increases.

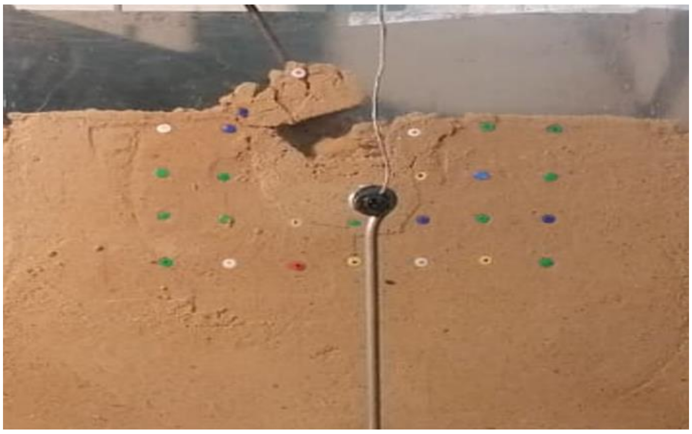

(a) Pure Sand

(b) Sand + 8% fines

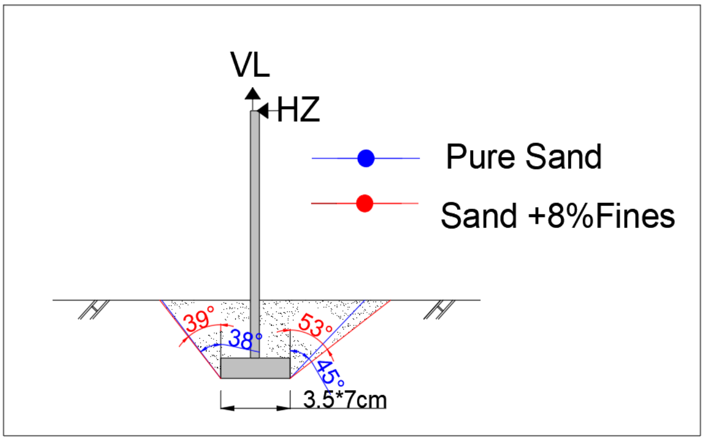

(c)

Fig. 28 (a), (b),(c). Failure mechanism for various soil types (pure sand and sand+8%fines) under vertical and horizontal force when (D/B) = 1 of the footing dim. (3.5*7) cm and (RC = 95%).

(a) Pure Sand

(b) Sand + 8% fines

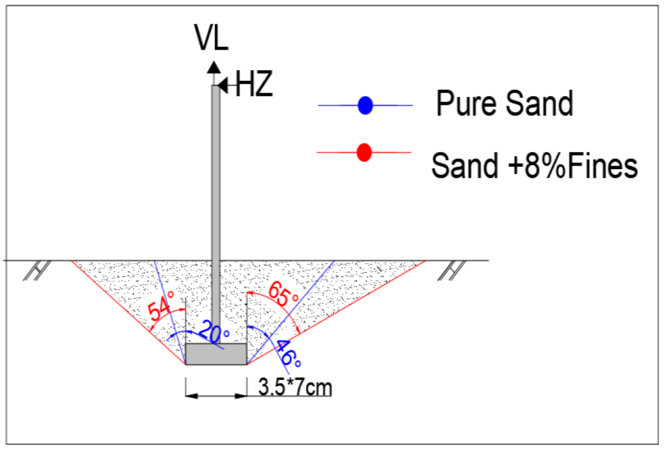

(c)

Fig. 29 (a),(b),(c). Failure mechanism for various soil types (pure sand and sand+8%fines) under vertical and horizontal force when (D/B) = 1.5 of the footing dim. (3.5*7) cm and (RC = 95%).

(a) Pure Sand

(b) Sand + 8% fines

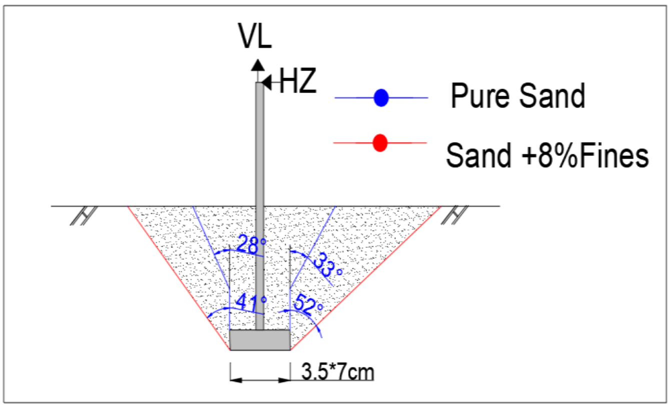

(c)

Fig. 30 (a),(b),(c). Failure mechanism for various soil types (pure sand and sand+8%fines) under vertical and horizontal force when (D/B) =2.5 of the footing dim. (3.5*7) cm and (RC = 95%).

(a) Pure Sand

(b) Sand + 8% fines

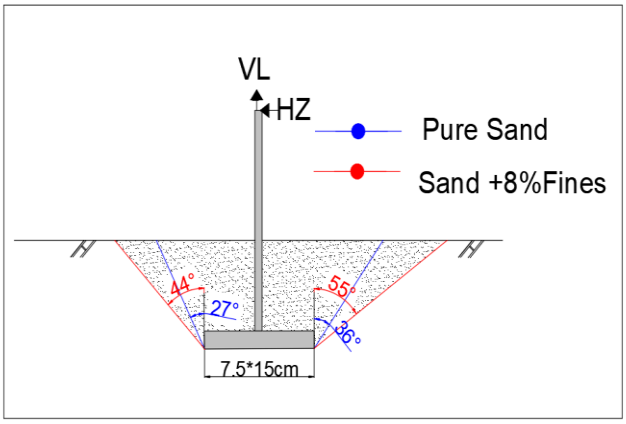

(c)

Fig. 31 (a),(b),(c). Failure mechanism for various soil types (pure sand and sand+8%fines) under vertical and horizontal force when (D/B) = 1 of the footing dim. (7.5*15) cm and (RC = 95%).

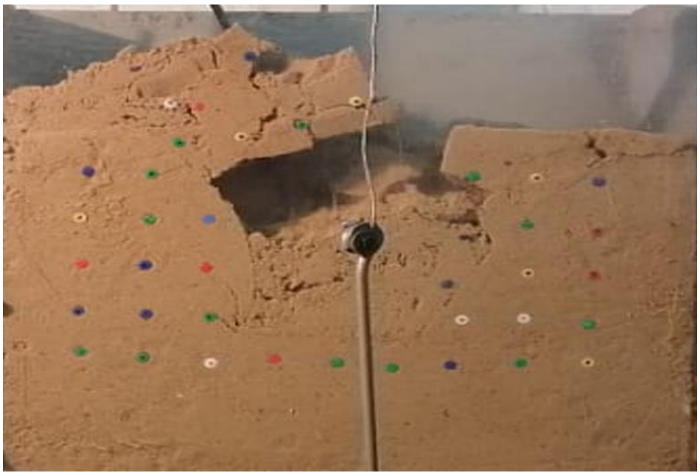

(a) Pure Sand

(b) Sand + 8% fines

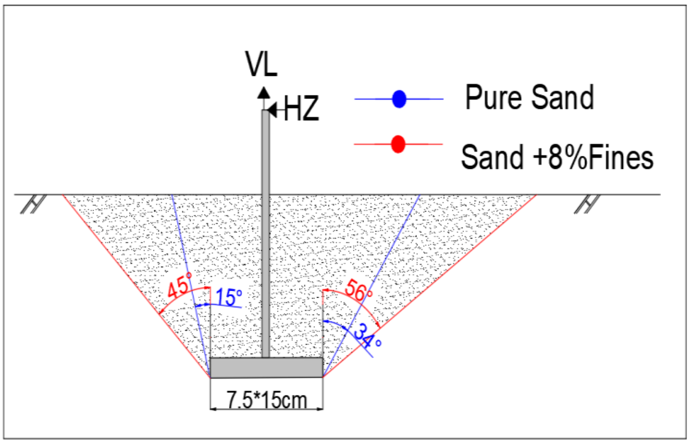

(c)

Fig. 32 (a),(b),(c). Failure mechanism for various soil types (pure sand and sand+8%fines) under vertical and horizontal force when (D/B) = 1.5 of the footing dim. (7.5*15) cm and (RC = 95%).

3. Conclusions

The conclusions obtained from this study can be summarized as follows:

- For single footings subjected to lateral and vertical forces, the final pullout force increases as the footings' embedment depth in the soil increases relative to their footing width.
- For single footings subjected to lateral and vertical forces, the final pullout force increases as the footings' embedment depth in the soil increases relative to their footing width.
- A change in embedded depth of footing-to-footing width up to 1.5 has no effect on the shape failure mechanism or the angle of inclination, but in the case of (D/B) = 2.5, it can be considered as a special case where as the failure mechanism is different, which is vertical then inclined by small angle.
- A rising percentage of fines the ultimate uplift resistance of single footings under uplift force was greatly enhanced. Therefore, adding fines to sandy soil at a percentage of at least 6% is advised.
- Adding fines to sandy soil does not effect on the failure rupture, but the value of the angle of inclination increase.
- The increase in the footing dimension leads to increase in the ultimate pullout force for single footing subjected to tension load and lateral load.
- The change of the dimensions of the footings does not affect the shape of the failure mechanism or the angle of inclination of the failure for single footing subjected to pullout force and lateral force.
- When single footing was subjected to pullout load and lateral load, the final pullout load increased as the relative compaction of the soil increased.
- The change in the relative compaction of soil does not affect the shape of the failure mechanism, but the value of the angle inclination increases by increasing the relative compaction of soil.

4. Recommendations for Future studies

- It is recommended to carry out the tests for the different footing groups dimensions with variable spacings center to center and compare the results of such a study to the results of the current research.

- It is recommended to study the effect of cyclic load on behavior of footings subject to pullout load and horizontal load.

- It is recommended to carry out (3-D) finite element analysis and compare results with the experimental results.

5. Reference

1. Adams J.I. and Hayes D.C. (1967), 'The Uplift Capacity of Shallow Foundation', Ontario Hydro Research Quarterly, Vol. 19, No. 1, pp. 1-13.
2. Balla A. (1961), 'The Resistance to Breaking Out of Mushroom Foundations for Pylons', Proc. 5th International Conference on Soil Mechanics and Foundation Engineering, pp. 569-576.
3. Banerjee S .and Mahadevuni N. (2017), 'Pull-Out Behaviour of Square Anchor Plates in Reinforced Soft Clay', Int. J. of Geosynth. and Ground Eng., pp 1-10.
4. Dickin E.A. and Laman (2007), 'Uplift Response of Strip Anchors in Cohesionless Soil', Journal of Advances in Engineering Software, Vol. 38, pp. 618-625.
5. Frydman S. and Shaham I. (1989), 'Pullout capacity of slab anchors in sand', Canadian Geotechnical Journal, Vol. 26, pp. 385-400.
6. Giffels W.C., Graham R.E. and Mook J.F. (1960), 'Concrete cylinder anchors proved for 345-KV tower line', Electrical World, Vol. 154, pp. 46-49.
7. Ireland H.O. (1963), 'Discussion on Uplift Resistance of Transmission Towers', by E.A. Turner, Journal of Power Division, ASCE, Vol. 89, No. 1, pp. 115-118.
8. Jyant Kumar K. (2004), 'Effect of dilatancy angle on uplift resistance of shallow foundation anchors', Indian Geotechnical Journal, Vol. 34, No. 2, pp. 203-225.
9. Korkmaz B. and Keskin M.S. (2017), 'Numerical Analysis of Uplift Capacity Behaviour of Circular Plate Anchors Under Different Conditions', Digital Proceeding of ICOCEE – CAPPADOCIA2017, Nevsehir, TURKEY, pp. 1-10.
10. Krishnaswamy N.R. and Parashar S.P. (1991), 'Effect of Submergence on the uplift resistance of footings with geosynthetic inclusion', Proceedings of Indian geotechnical conference, Surat, India, pp. 333-336.
11. Meyerhof G.G. and Adams J.I.(1968), 'The Ultimate Uplift Capacity of Foundations', Canadian Geotechnical Journal, Vol. 5, No. 4, pp. 225-244.
12. Meyerhof, G. G. (1973a). 'The Uplift Capacity of Foundations under Oblique Loads', Canadian Geotechnical journal, Vol. 10, pp. 64-70.
13. Mors H. (1959), 'The behaviour of mast foundations subject to tensile forces', Bautechnik, Vol. 10, pp. 367-378 (as reported by Balla 1961).
14. Niroumand, H., Kassim, K.A. (2013a), 'Uplift of Symmetrical Anchor Plates by Using Grid-Fixed Reinforced', China Ocean Eng., Vol. 28, No. 1, pp. 115 – 126.
15. Sutherland H.B. (1965), 'Model studies for shaft raising through cohesionless soils', Proc. 6th Int. Conf. Soil Mechanics and Foundation Engineering, Montreal, Vol. 2, pp. 410-413.
16. Turner E.A. (1962), 'Uplift resistance of transmission tower footings', Journal of Power Division, ASCE, Vol. 88, pp. 17-32.